Excess Electrochemical Vaporization of SiO from Na₂O-SiO₂ Molten Slag by Transfer Thermal Plasma of Ar

Keiichirou Kashimura, Kuniyoshi Nakada and Kazuhiro Nagata

Department of Chemistry and Materials Science, Tokyo Institute of Technology, Tokyo 152-8552, Japan

Transfer thermal plasma of argon (Ar) was applied onto the surface of 25 mol% Na₂O-SiO₂ molten slag using a hybrid plasma furnace composed of non-transfer and transfer thermal plasma. A tungsten rod was used as an electrode. The flame from the transfer plasma spread over the surface of the slag. The direct current of the transfer plasma was a maximum just after ignition and then decreased. When the transfer plasma was applied with a voltage less than 80 V, the iron dissolved and diffused into the molten slag as Fe^{2+} at the iron plate anode electrode according to Faraday's law. For voltages over 90 V, oxygen gas bubbles evolved at the anode in addition to iron dissolution. SiO gas vaporized more than sodium (Na) gas from the slag surface, although the opposite phenomena should take place thermodynamically and kinetically. Furthermore, the quantity of SiO gas was 10 to 100 times more than that expected from Faraday's law. [doi:10.2320/matertrans.MRA2008003]

1. Introduction

When incinerator ash is melted in a furnace of transfer thermal plasma, it is reported that lead and zinc selectively evaporate from molten slag.[1,2] The evaporation of these metals is thought to be caused by high temperature plasma. The evaporation mechanisms are not clear but are known to be complicated due to physical aspects such as electro-magnetic fields. To-date, researchers have been assumed that the selective vaporization is due to electrochemical reactions at the interface between the slag and plasma flame. Molten slag is an electrolyte and plasma acts as a cathode electrode. Mobile cations such as Ca^{2+}, Na^+ and K^+, in molten silicate slag carry electric current, while metal ions such as zinc and lead ions are reduced to metal vapor by electrons in the transfer thermal plasma at molten slag surface. Thermal plasma in non-equilibrium consists of weakly dissociated ions and electrons. Electron in transfer thermal plasma is of low density and has a high kinetic energy under large electric fields, while there is a high density of electrons in the metal electrode of an electrochemical cell, having low kinetic energies. This analogy indicates that lead and zinc ions in molten slag are electrochemically reduced by electrons in the transfer plasma at the slag/plasma interface.

In this study, the electrochemical reactions at the interface of molten silicate and transfer plasma were examined using a simple system of 25 mol% Na₂O-SiO₂ slag and transfer thermal plasma of Ar.

2. Experiment

A 20 kW hybrid plasma arc furnace shown in Fig. 1 was employed. The hybrid plasma jet was composed of a non-transfer plasma of Ar gas (99.999%) and a transfer plasma between a tungsten electrode and a water cooled copper (Cu) stand.

A sample of 25 mol% Na₂O-SiO₂ slag was prepared from a mixture of NaCO₃ and SiO₂ reagent powders. The slag was premelted in air using a platinum crucible, quenched on a water cooled Cu plate and crushed.
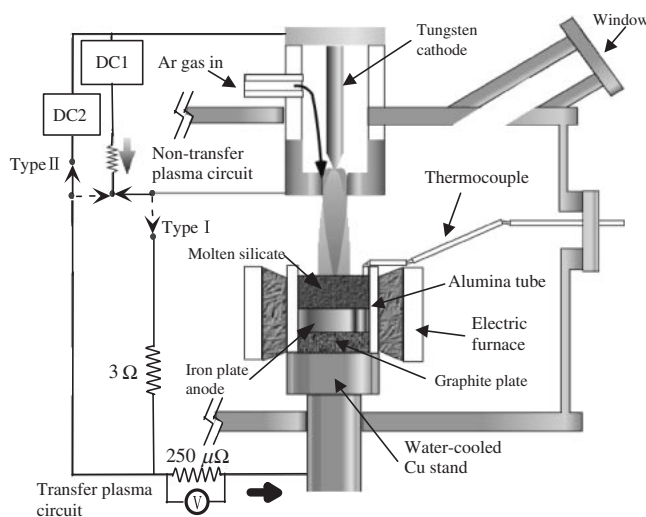

Fig. 1 Schematic illustration of a 20 kW hybrid plasma arc furnace. The transfer plasma was generated using 2 electric circuits. Type I: automatic generation with a direct current of 200 A (DC1) and Type II: generation using a potentiostadt (DC2) after igniting the non-transfer thermal plasma with a current of 150 A (DC1).

A polished iron plate with an inside diameter of 28 mm and thickness of 5 mm was fixed onto the bottom of alumina tube. The sample of slag was put in the crucible of the alumina tube. The crucible was set onto a water-cooled Cu stand with a graphite plate (28 mm diameter and 25 mm thickness) as an electric connector and thermal insulator. The crucible was heated using an electric resistance furnace in the chamber.

The chamber was evacuated and rinsed with Ar gas. After then, Ar gas was passed through the plasma gun with a flow rate of 3 to 5 l/min at one atmosphere pressure. The slag was melted by the resistance furnace and kept at 1200 K for 2 h in order to make complete contact with the iron plate. The temperature of the slag was measured at the molten slag surface near crucible wall using a R-type thermocouple insulated with fine alumina tubes. The distance between tungsten electrode and slag surface was controlled by the vertical movement of the Cu stand.

Table 1 Experimental conditions.

No.	Weight of slag(g)	Ar flow rate(l/min)	Electrode Gap(mm)	Type	Voltage (V)	Reaction time(min)
1	6.3869	5.0	23.5	I	—	15
2	7.0316	5.0	25.4	I	—	2
3	5.9870	5.0	29.0	I	—	10
4	5.1147	5.0	35.6	I	—	6
5	4.8188	5.0	27.1	I	—	1
6	3.8384	5.9	25.0	I	—	9
7	4.9624	4.1	—	I	—	11
8	5.8186	3.0	35.0	I	—	6
9	5.2837	5.0	33.0	II	0	30
10	4.9050	5.0	32.6	II	0	15
11	5.0777	4.0	29.0	II	0	30
12	4.8442	4.3	32.3	II	50	2
13	6.1093	5.0	—	II	50	11
14	7.0974	5.0	32.5	II	70	10
15	6.8975	5.0	27.3	II	90	10
16	7.3155	5.0	30.9	II	90	10
17	7.1174	5.0	39.0	II	90	10
18	7.1423	5.0	26.0	II	90	10
19	7.1120	5.0	22.2	II	80	10
20	7.5526	5.0	31.0	II	40	10
21	8.0042	5.0	30.0	II	80	10

Note: The voltage of transfer plasma was not fixed in Type I but controlled in Type II from 0 to 90 V by a potentiometer.

The transfer thermal plasma was generated using two electrical circuits. Type I: After the non-transfer thermal plasma was ignited with a direct current of 200 A (DC1) under flowing Ar gas, the transfer thermal plasma was automatically generated when the electrical resistance between tungsten electrode and iron plate became less than 3 Ω. Type II: After igniting the non-transfer thermal plasma with a current of 150 A (DC1), a constant voltage was applied between the tungsten electrode and iron plate by a potentiostat (DC2) and the transfer plasma was easily generated.

The experimental conditions are shown in Table 1. The electric current and voltage of the transfer and non-transfer plasmas were recorded using a computer. The plasma near the slag surface was monitored from a window by a video camera and the spectrum of plasma was analyzed by an optical fiber spectrometer (USB2000, Ocean Optics) with a slit width of 5 μm and wavelength range of 250 to 800 nm. The spectroscopy was calibrated using a Hg-Ar lamp.

The concentration distributions of Na, Si and Fe in the slag samples after experiments were determined by EPMA (Electron Probe Micro Analyzer, Shimazu Co.). The composition of the slag samples before and after experiments was analyzed by ICP-AES (Inductively Coupled Plasma-Atomic Emission Spectrometry). Powder adhered under the lid of the chamber after experiments was also analyzed. The compounds in the slag samples were identified using X-ray Diffractometer (Rint-TTR-3C/PC, Rigaku Denki). The chemical state of Fe, Si, Na and oxygen in slag
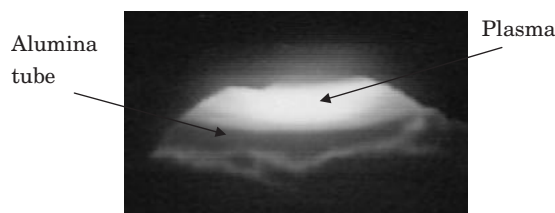

Fig. 2 Transfer thermal plasma flame of Ar which has spread over the molten silicate surface.

was measured by XPS (X-ray Photoelectron Spectroscopy) using Mg as a standard.

3. Results

Figure 2 is a photograph of the transfer thermal plasma flame which has spread over the molten slag surface. The plasma was yellow. The color of the non-transfer plasma without transfer plasma was purple or blue by Ar gas. On the other hand, when iron metal was melted, the transfer plasma was concentrated to a hot spot on the metal surface and was a brilliant white color. The spreading flame of plasma on the slag showed the plasma to be uniformly covering the whole surface of the slag.

As shown in Fig. 3, in the case of the Type I circuit (Run No. 5), the current of the transfer plasma initially increased to about 1.5 A and then rapidly decreased to about 10 mA when the current of non-transfer plasma was about 10 A. In the case of the Type II circuit (Run No. 13), when a constant voltage of 50 V (DC2) was applied by the potentiometer, the current initially increased to 0.9 A and then rapidly decreased to about 10 mA. The current and voltage of the non-transfer plasma were 20 to 40 A and 20 V (DC1), respectively. When the transfer plasma with a voltage of 90 V (DC2) was applied (Run No. 18), the current and voltage of the transfer plasma oscillated around 0.9 A and 60 V (DC1), respectively.

As shown in Fig. 4, the temperature of the molten slag during the application of the transfer plasma gradually decreased by 100 K for Run No. 5 of Type I. When the plasma flame was unstable, the temperature peaked sharply. The temperature decrease was caused by the current decrease of the non-transfer plasma for Type I when a part of the current was consumed by the transfer plasma. For Run 20 of Type II, the temperature increased to about 1400 K and then gradually decreased to 1300 K. The current of the non-transfer plasma for Type II remained constant during the supply of additional current of the transfer plasma.

From the spectrum of the transfer plasma on the slag surface (Run No. 15), the activated species of Na, Ar, and Si and neutral oxygen were detected, as shown in Fig. 5. The intensity of Na at 589 nm was very strong even at low concentration.

The powder that adhered on the lid of chamber (Run No. 18) was black. ICP analysis showed that powder with a mass of 15.1 mg included 0.23 mg of Na, 5.0 mg of Si and 2.5 mg of Fe. XRD analysis showed the Na and Si to be metallic.

The surface of the slag had a dented shape after cooling to room temperature. The depth of the slag at the center was
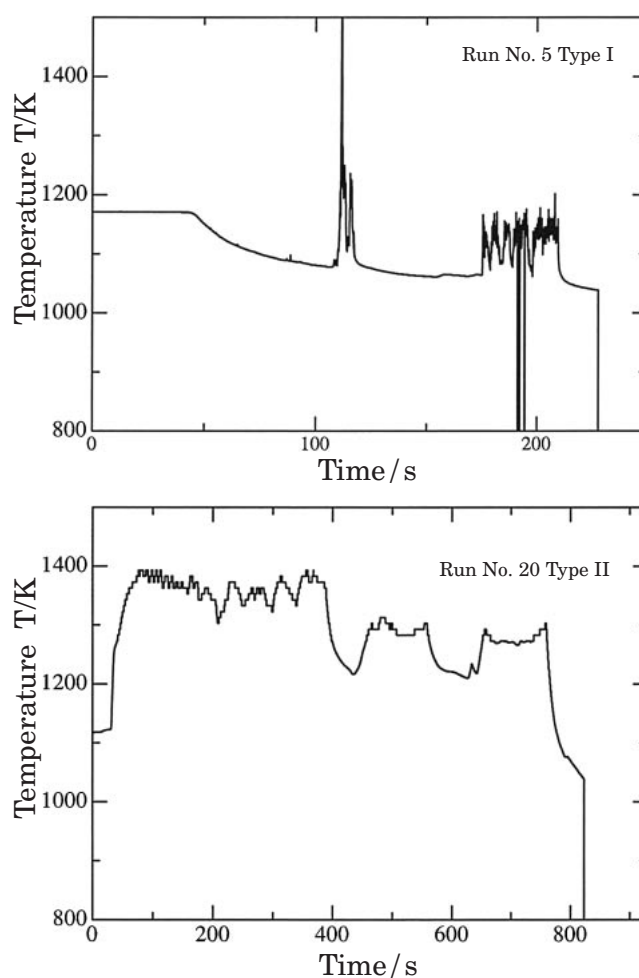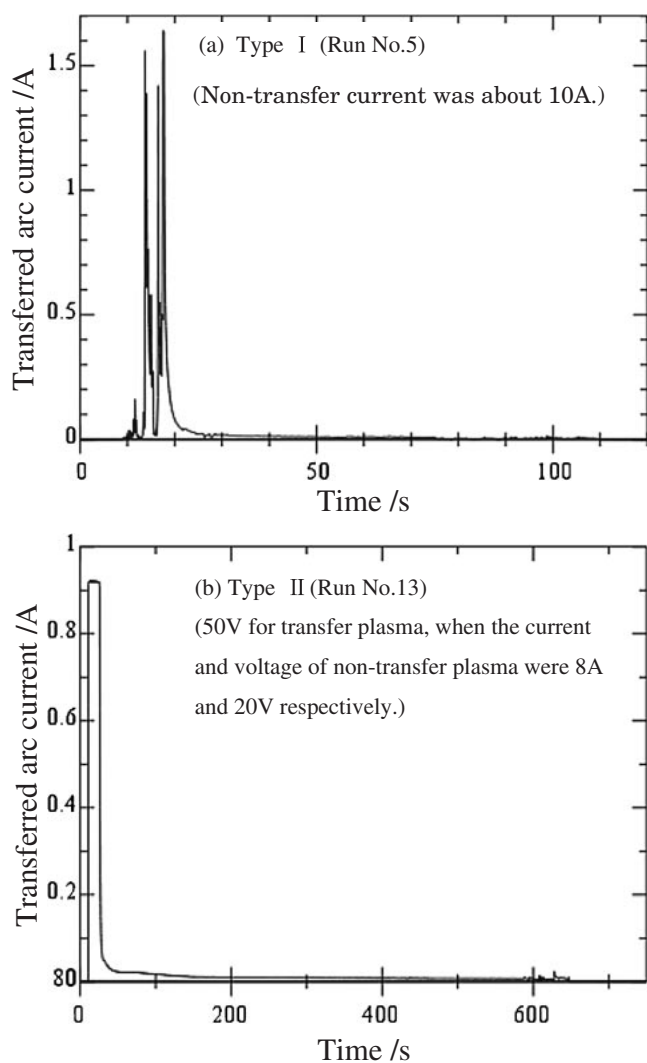
Fig. 3   (a) Current of transfer thermal plasma in the cases of Type I (a) and Type II (b).

Fig. 4   Temperature of molten slag during the application of the transfer thermal plasma using Type I and Type II electric circuits.
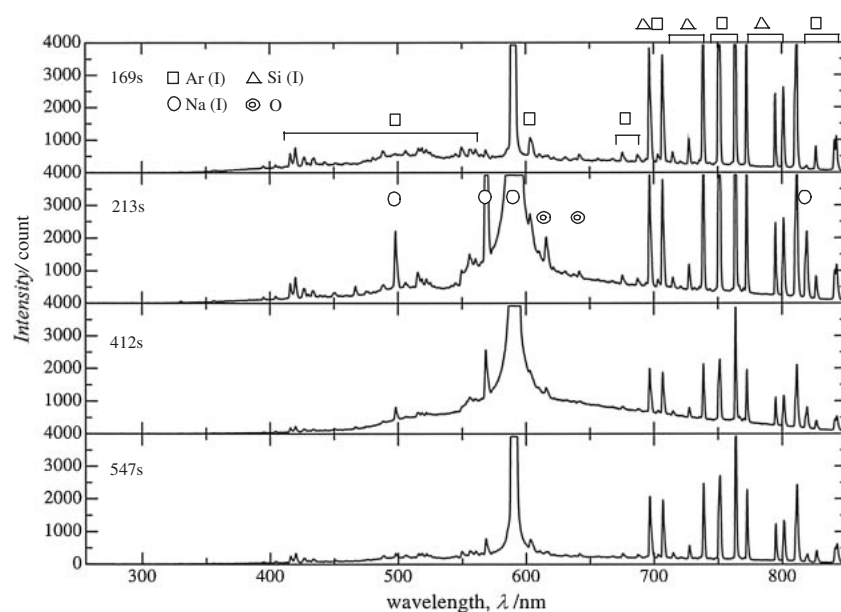
Fig. 5   Spectrum of the transfer thermal plasma of Ar on the surface of molten silicate slag. (Run No. 15), Time is progress in generating transfer plasma. Integration time is 100 ms.

Table 2 Bonding Energy of elements at different positions in slag measured by XPS.

Position	Bonding Energy (eV)			
	Fe(2p)	Si(2p)	Na(1s)	O(1s)
surface	—	102.2	1072.1	531.6
middle	709.4	102.5	1072.0	532.0
Fe/slag interface	709.4	102.6	1071.9	532.1

Note: Reference data;[6] Fe(2p) in Fe:707.0, 706.7, 706.8, FeO:709.4, Fe_3O_4:708.2, 710.4, Fe_2O_3:710.8, Si(2p) in Si:99.5 and SiO_2(quartz): 103.7, Na(1s) in Na:1071.8 and 1071.4 and Na_2O:1072.5 and O(1s) in SiO_2(quartz):532.7, 533.2.

Table 3 Composition of slag before and after reaction.

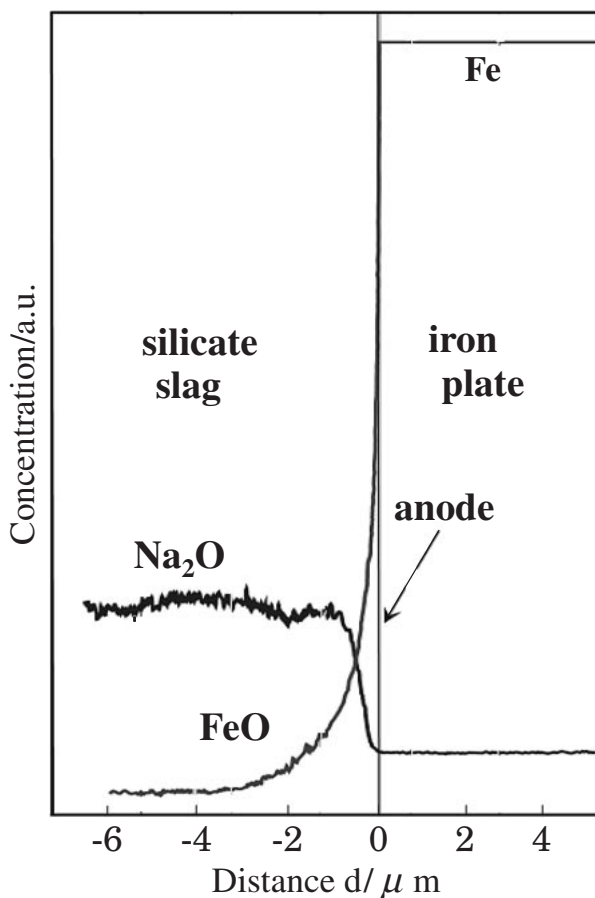| No.	Initial composition (mol%)			Final composition (mol%)			Voltage*
	Na/Si	Na_2O	SiO_2	Na/Si	Na_2O	SiO_2	(V) (Type)
1	0.573	22.27	77.73	0.689	25.61	74.39	— (I)
2	0.573	22.27	77.73	0.727	26.59	73.41	— (I)
3	0.575	22.33	77.67	0.646	24.41	75.59	— (I)
4	0.575	22.33	77.67	0.678	25.32	74.68	— (I)
5	0.575	22.33	77.67	0.592	22.85	77.15	— (I)
6	0.575	22.33	77.67	0.660	24.82	75.18	— (I)
7	0.575	22.33	77.67	0.653	24.62	75.38	— (I)
9	0.639	24.20	75.80	0.592	22.84	77.16	0 (II)
10	0.639	24.20	75.80	0.617	23.58	76.42	0 (II)
11	0.639	24.20	75.80	0.603	23.16	76.84	0 (II)
12	0.639	24.20	75.80	0.636	24.20	75.80	50 (II)
13	0.572	22.25	77.75	0.588	22.71	77.29	50 (II)
14	0.649	24.50	75.50	0.663	24.90	75.10	70 (II)
15	0.592	22.83	77.17	0.443	18.14	81.86	90 (II)
17	0.580	22.49	77.51	0.515	20.48	79.52	90 (II)
18	0.580	22.49	77.51	0.544	21.38	78.62	90 (II)
20	0.558	21.80	78.20	0.558	21.82	78.18	40 (II)
21	0.593	22.87	77.13	0.616	23.56	76.44	80 (II)

Note: *: the voltage of DC2 in Fig. 1.

Fig. 6 Diffusion profiles of FeO and Na_2O into the molten slag from the iron plate. These profiles were estimated from X-ray intensities of Fe and Na in silicate slag (Run No. 4).

about 4 mm and that near the wall of crucible was about 10 mm. The slag samples were cut through the center of the crucible and their cross sections were analyzed.

Table 2 shows the XPS results and the bonding energies of elements[3] in slag (Run No. 15) at different positions over the surface, middle and interface with iron plate. Iron existed as Fe^{2+} ion in the middle and near the interface. Iron ions near the slag surface were not detected because of too dilute a concentration. Si, Na and oxygen existed in silicate slag.

Figure 6 shows the diffusion profile of FeO into the molten slag from the iron plate (Run No. 4). The diffusion phenomena appeared in cases of Type I and Type II with less than 50 V (DC2) for the transfer plasma. A voltages of more

than 50 V in Type II, oxygen gas bubbles with diameters of 100 to 200 μm were generated at the interface of the iron plate anode and the slag. In the case of Type II with 90 V (Run No. 15), compounds of SiO_2, Fe_3O_4 and Fe_2SiO_4 were detected in the slag layer with the thickness of 100 μm on the iron plate anode electrode.

The composition of the slag before and after the reactions are listed in Table 3. The composition ratio of Na to Si in slag increased after the experiments of Type I. In the case of Type II, the ratio decreased for 0 V of the voltage of the transfer plasma. It did not change for 40 V but increased for 50 V and 70 V. The ratio however, decreased again for 90 V.

4. Discussion

4.1 Electrochemical reactions at the slag surface

The vapor pressures of Na and SiO in equilibrium with 25 mol% Na_2O-SiO_2 molten slag were calculated from the standard Gibbs energy of formation of Na_2O and SiO_2,[4] the activity of Na_2O and SiO_2 in the slag and the oxygen partial pressure in the atmosphere. The activity of Na_2O and SiO_2 were 2.5×10^{-9} and 0.15 at 1473 K,[5] respectively. The variation of the activity coefficient of the oxide in silicate slag on temperature was small. When the partial pressure of oxygen was 1×10^{-4} atm in Ar, P_{Na} and P_{SiO} were 2.7×10^{-9} atm and 5.6×10^{-21} atm at 1200 K and 2.2×10^{-8} atm and 2.6×10^{-18} atm at 1300 K, respectively. Psi was very small with a value of 1.1×10^{-47} atm. For the partial pressure of oxygen of 1×10^{-16} atm in equilibrium with Fe and FeO, P_{Na} and P_{SiO} were 2.7×10^{-6} atm and 2.6×10^{-18} atm, respectively. The flux of evaporated gas was proportional to the partial pressure of gas and inversely

Table 4   The quantity of electricity calculated from the amounts of SiO$_2$ decrease and FeO dissolution in slag according to the Faraday's law in comparison with the measured one from electric current.

No.	Cathode reaction		Anode reaction		Quantity of electricity$^+$/C	Voltage /V (Type)
	SiO/10^{-3} mol	Q*/C	Fe^{2+}/10^{-3} mol	Q$^{\#}$/C		
1	9.263	1788	0.4026	77.7	—	— (I)
2	15.182	2930	0.3788	73.1	—	— (I)
3	15.890	3067	0.4284	82.7	—	— (I)
4	9.989	1928	0.7972	153.9	142.0	— (I)
5	1.826	352	0.1015	19.6	13.0	— (I)
6	6.378	1233	0.1387	26.8	18.0	— (I)
7	8.100	1563	0.3796	73.3	—	— (I)
12	0.000	0	0.0377	7.3	6.3	50 (II)
13	2.047	395	0.2514	48.5	21.2	50 (II)
14	1.885	364	0.1216	23.5	30.7	70 (II)
20	0.106	21	0.0635	12.3	11.8	40 (II)
21	3.877	748	0.1509	29.1	39.4	80 (II)

Note: Q* and Q$^{\#}$ are calculated from the amount of SiO$_2$ decrease in slag at cathode and FeO dissolution at anode according to the Faraday's law, respectively. +: Quantity of electricity is measured from the integration of electric current with reaction time.

proportional to the square root of the molecular weight of gas according to the Langmuir's hypothesis.[6] The molecular weight of Na is 23 and that of SiO is 44. Thus, Na evaporates 6×10^{11} times greater than SiO. Thermodynamic and kinetic calculations show that the quantity of Na and SiO vapor is very small and that Na vaporizes more than Si. When only the non-transfer plasma was applied onto the slag surface, that is 0 V of the voltage for transfer plasma, the composition ratio of Na to Si in slag decreased a little after the experiments.

For the transfer plasma with voltages from 40 V to 80 V (DC2), the ratio increased. At the slag surface, electrons from the transfer plasma react with molten slag according to the cathode reaction,

$$SiO_2(\text{in slag}) + 2e(\text{plasma}) \rightarrow SiO(\text{gas}) + O^{2-}(\text{in slag}) \quad (1)$$
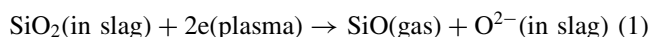
For 90 V of DC2, the additional reaction takes place,

$$Na^+(\text{in slag}) + e \rightarrow Na(\text{gas}) \quad (2)$$

and as experimental results show that metallic Si evaporated above the surface, the SiO is probably reduced by electrons in plasma,

$$SiO(\text{gas}) + 2e(\text{plasma}) \rightarrow Si(\text{plasma}) + O^{2-}(\text{plasma}) \quad (3)$$
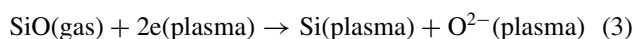
In this case, the ratio of Na to Si in the slag composition decreases after experiments.

4.2   Electrochemical dissolution of Fe at the anode electrode

At the interface of the iron plate and slag, the iron electrochemically solved into molten slag as Fe^{2+} and oxygen gas evolved for voltages more than 50 V. The anode reactions are,

$$Fe \rightarrow Fe^{2+} + 2e \quad (4)$$
$$O^{2-} \rightarrow 1/2O_2 + 2e \quad (5)$$
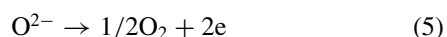
For 90 V of DC2, the SiO$_2$, Fe$_3$O$_4$ and Fe$_2$SiO$_4$ compounds were produced because of the lack of Na$^+$ ions.

4.3   Excess evaporation of SiO

From the amount of dissolved Fe^{2+} in the molten slag at the anode electrode, the quantity of electricity was calculated according to Faraday's law. Table 4 shows the calculated quantity of electricity in comparison with that obtained from the integration of electric current passed through the molten slag with reaction time. In Type I and Type II, with a transfer plasma voltage of 40 and 50 V (DC2), the quantity of electricity calculated from Fe^{2+} was slightly larger than that obtained from the electric current. This error is due to the unstable electric current as shown in Fig. 3. With 70 and 80 V, the calculated quantity of electricity was smaller than the value from the electric current because of the additional reactions due to oxygen gas evolution.

On the other hand, at the cathode of the slag surface, the quantity of electricity was calculated from the decrease of SiO$_2$ in molten slag according to Faraday's law. It was assumed that Na did not evaporate. The quantity of electricity was 10 to 100 times more than that measured from the electric current, as shown in Table 4. The deviation from Faraday's law is clearly seen in Fig. 7. The excess cathode reaction at the plasma/slag interface was caused by bombardment of excess electrons in the transfer plasma on the slag surface.

4.4   Charge balance for excess evaporation of SiO

The excess evaporation of SiO from the slag surface should be compensated by other reactions for maintaining electro-neutrality. The most probable reaction is the emission of O^{2-} ions from slag to plasma,

$$O^{2-}(\text{slag}) \rightarrow O^{2-}(\text{plasma}) \quad (6)$$
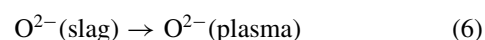
and O^{2-} reacts with Ar$^+$ in the plasma phase near the slag surface,

$$O^{2-} + 2Ar^+ \rightarrow O + 2Ar \quad (7)$$
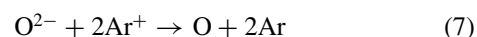
The spectrum of the plasma near the slag surface showed the existence of neutral oxygen O, as well as activated Na, Si
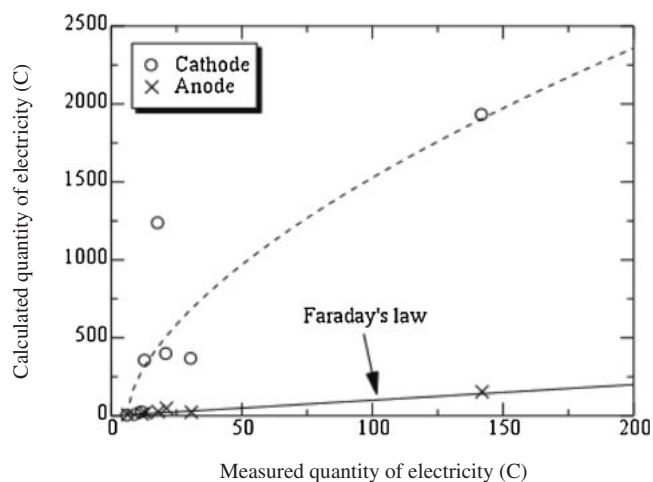
Fig. 7　Quantity of electricity obtained from the decrease of SiO_2 (cathode) and the dissolution of FeO (anode) in molten slag according to Faraday's law in comparison with that obtained from the integration of electric current passed through the molten slag with reaction time.

and Ar. Ar^+ ions dissociated with electrons in the plasma phase were blown onto the slag surface by the Ar gas flow. Excess electrons in the plasma bombarded the slag surface and charged the surface negatively. The Ar^+ ions in the plasma were attracted near to the surface to produce a double layer.

5. Conclusions

Transfer thermal plasma of Ar was applied onto the surface of 25 mol% Na_2O-SiO_2 molten slag at 1200 K. SiO gas electrochemically evaporated from the surface, although the vaporization rate of Na should be larger than that of SiO from thermodynamic and kinetic calculations. Also, the amount of vaporized SiO was more than that calculated from Faraday's law, while the amount of iron dissolution at the iron plate anode followed this law. The excess vaporization of SiO was caused by the bombardment of excess electrons in the transfer plasma onto the slag surface. In order to maintain electro-neutrality, it was assumed that O^{2-} ions were emitted from the slag surface to the plasma.

REFERENCES

1) C. Izumikawa: Waste Management **16** (1996) 501.
2) H. Jimbo, *et al.*: Proc. 1st Asia-Pacific Intern. Symp. on the Basic of Plasma Technology, 1997, Taiwan.
3) J. F. Moulder, W. F. Stickle, P. E. Sobol and K. D. Bomben: *Handbook of X-ray Photoelectron Spectroscopy*, ed. by J. Chastain and R. C. King, Jr., (Ohysical Electronics, Inc., 1995).
4) M. W. Chase, Jr.: *NIST-JANAF Thermochemical Tables, 4th ed., Part II*, (Amer. Ceram. Soc., 1998).
5) S. Yamaguchi, A. Imai and K. S. Goto: J. Jpn. Inst. Met. **25** (1984) 879.
6) I. Langmuir: Phys. Rev. **2** (1913) 329.